(5) J. A. Dilts and D. F. Shriver, *J. Am. Chem. Soc.*, **90**, 5769 (1968).
(6) S. A. Bezman, M. R. Churchill, J. A. Osborn, and J. Wormald, *J. Am. Chem. Soc.*, **93**, 2063 (1971).
(7) G. Monnier, *Ann. Chim. (Paris)*, **2**, 14 (1957).
(8) E. C. Ashby and R. Kovar, *Inorg. Chem.*, **16**, 1437 (1977).
(9) E. C. Ashby, T. F. Korenowski, and R. D. Schwartz, *J. Chem. Soc., Chem. Commun.*, 157 (1974).
(10) E. C. Ashby and R. D. Schwartz, *J. Chem. Educ.*, **51**, 65 (1974).
(11) D. F. Shriver, "The Manipulation of Air Sensitive Compounds", McGraw-Hill, New York, N.Y., 1969.
(12) G. B. Kauffman and L. A. Teter, *Inorg. Synth.*, **7**, 9 (1963).
(13) S. Aronson and F. J. Salzano, *Inorg. Chem.*, **8**, 1541 (1969).
(14) In a separate study we have determined the Al–H stretching absorption of $LiAl(CH_3)H_3$, $LiAl(CH_3)_2H_2$, and $LiAl(CH_3)_3H$ in Et_2O and THF by reacting $LiAlH_4$ with $LiAl(CH_3)_4$. Clearly as the stoichiometry of the reaction is varied, the Al–H stretching frequency of one compound disappears and a different Al–H frequency appears representing the next redistribution analogue. The Al–H stretching frequency of the above compounds in Et_2O and THF is as follows: 1728, 1708, and 1685 cm^{-1} in Et_2O and 1685, 1678, and 1665 cm^{-1} in THF, respectively.

Contribution from the Department of Chemistry, Purdue University, West Lafayette, Indiana 47907

Kinetics and Mechanisms of the Copper-Catalyzed Decomposition of Hypochlorite and Hypobromite. Properties of a Dimeric Copper(III) Hydroxide Intermediate

EDWARD T. GRAY, JR., RICHARD W. TAYLOR, and DALE W. MARGERUM*

Received June 22, 1977 AIC70448Y

Copper(II) hydroxide complexes catalyze the decomposition of OCl^- and OBr^- via two pathways, one first order and one second order in copper. The latter pathway produces small amounts of a yellow intermediate, B, which is a dimeric copper(III)

$$OX^- \xrightarrow[Cu(II)]{k_{AB}} B \xrightarrow{k_{BC}} {}^1/_2O_2 + X^- \qquad k_{BC} >> k_{AB}$$

hydroxide complex. The spectrum of this complex has maxima at 270 and 362 nm (each with $\epsilon \sim 18\,800\ M^{-1}\ cm^{-1}$). Chloride has no effect on reactions of OCl^-. Bromide suppresses both the concentration of B and the rate of oxygen evolution during the decomposition of OBr^- because of the reversibility of the formation of B. This is used to establish the stoichiometry of the dimer and its electrode potential: $Cu^{III}_2(O)(OH)_7^{3-} + H_2O + 2e^- \rightarrow 2Cu^{II}(OH)_4^{2-} + OH^-$; $E^\circ = 0.82$ V (vs. NHE). The half-life of this dimer (producing oxygen) is 10.5 s in 1 M NaOH at 25 °C. The monomeric pathway does not produce measurable amounts of Cu(III).

Introduction

The addition of Cu(II) to alkaline solutions of hypochlorite or hypobromite results in the formation of a yellow species and the evolution of oxygen. Thenard,[1] in 1818, was the first to report this behavior in the case of hypochlorite. He suggested that the yellow species was copper peroxide. In 1953, Lister[2] claimed that the yellow species could not be a peroxide because of the rapid decomposition of peroxides by hypochlorite. He proposed that it was a copper(III) hydroxide complex, $Cu(OH)_4^-$. This formula was based on conclusions from a rough solubility study as a function of OH^-. The ability of earlier workers to precipitate red $Ba(CuO_2)_2$ from hypobromite solutions[3,4] was evidence for the existence of a copper(III) oxide salt. In 1965, Magee and Wood[5] isolated solid sodium dioxocuprate(III) ($NaCuO_2$) from alkaline solutions of OBr^- and Cu(II). Despite this, they challenged Lister's interpretation concerning the presence of an appreciable amount of a soluble copper(III) hydroxide complex. Their experiments showed the reddish brown $NaCuO_2$ to be unstable in alkaline solution and to decompose as shown in eq 1. They suggested

$$4NaCu^{III}O_2 + 2H_2O \rightarrow 4NaOH + 4Cu^{II}O + O_2 \qquad (1)$$

Lister's results could be explained by assuming that most of the copper was present as a copper(II) hypochlorite complex and only a small fraction was present as Cu(III).

The ability of copper to catalyze the decomposition of OCl^- (eq 2) is not under dispute, but there is disagreement about

$$2OCl^- \xrightarrow{Cu(II)} O_2 + 2Cl^- \qquad (2)$$

the reaction order. Lister reported the order dependence in Cu(II) to be 1.0 while Prokopcikas[6] found it to be 2.0. In the analogous OBr^- decomposition, Sakharov[7] found a $[Cu(II)]^{1.7}$ order dependence.

In the present work, the kinetics of the copper-catalyzed decomposition of hypohalite ions in strong base are investigated. The reaction order in copper varies with the concentration of Cu(II) because of the existence of two reaction pathways. Confirmation of a reactive Cu(III) complex in solution is presented. The stoichiometry, absorption spectrum, electrochemical potential, and reactivity are determined for the Cu(III) complex.

Copper(II) hydroxide is slightly amphoteric and redissolves in strong base to form $Cu(OH)_3^-$ and $Cu(OH)_4^{2-}$ complexes.[8] As the present work shows, copper(III) hydroxide complexes are not very stable in basic solution but do have a finite lifetime. Two Cu(III) complexes containing oxygen donor groups, which have long been known to exist in basic solution, are those of periodate and tellurate.[9,10] Their stability and oxidizing power have been used by Beck[11-13] and others[14] in a number of analytical determinations. Crystalline $Na_3KH_3[Cu(IO_6)_2]\cdot 14H_2O$ has four periodate oxygen atoms in a square plane around Cu(III) at a distance of 1.9 Å and a water molecule forming a fifth bond to copper at a distance of 2.7 Å.[15]

Other donor groups also are effective in stabilizing Cu(III), particularly deprotonated-nitrogen peptide donors which have been shown to form relatively stable complexes in solution.[16-18] In somewhat earlier work, electrochemical oxidation was used to prepare Cu(III) complexes of macrocyclic tetramines in acetonitrile.[19] Pulsed-radiolysis studies produced extremely reactive Cu(III) complexes of amines and amino acids in aqueous solution.[20] Solid Cu(III) complexes of biuret and of oxamide have been isolated and characterized.[21,22] The

high-spin octahedral complex K_3CuF_6[23] can be prepared by fluorination of $KCl/CuCl_2$ mixtures. A crystal structure analysis also has been reported for copper(III) dithiocarbamate bromide.[24]

Experimental Section

Reagents. Copper(II) perchlorate was prepared by neutralization of cupric carbonate with perchloric acid and was purified by recrystallization from water. A stock solution was standardized iodometrically with thiosulfate titrant using starch as an indicator (electrolytic copper foil was used as a primary standard) and by EDTA titration with murexide indicator.[25]

Sodium hydroxide solutions were freshly prepared from electrolytic pellets. These solutions were standardized with perchloric acid using both phenolphthalein and methyl orange indicators to verify the lack of appreciable carbonate contamination.

Reagent grade sodium hypochlorite was used without further purification. Sodium hypobromite was prepared either by the reaction of sodium bromide with sodium hypochlorite or by the hydrolysis of reagent grade bromine with sodium hydroxide. The resulting NaOBr solutions were stored under refrigeration in order to retard disproportionation. Hypochlorite and hypobromite solutions were standardized spectrophotometrically at 292 nm (ϵ 350 M^{-1} cm^{-1}) and 329 nm (ϵ 343 M^{-1} cm^{-1}), respectively.[26]

Measurements. Fast reactions of Cu(II) with the hypohalites were monitored with a Durrum stopped-flow spectrophotometer interfaced to a Hewlett-Packard 2115A computer.[27] Reactions with OCl^- were monitored at 400 or 475 nm and those with OBr^- were monitored at 400 nm. Rapid-dilution experiments were studied at 362 nm using a Cary 14 spectrophotometer or a modified Beckman DU spectrophotometer. The signal from the DU photomultiplier was recorded using a Biomation 8100 transient recorder which was interfaced to a Hewlett-Packard 2100 computer. Slower reactions of Cu(II) with OCl^- and OBr^- were studied at 340–355 and 375 nm, respectively, using a Cary 16 spectrophotometer.

Optical spectra of the intermediate species formed by the reaction of Cu(II) with OCl^- and OBr^- were obtained using a rapid-scanning spectrophotometer employing a vidicon tube as the detector.[28] The output of the vidicon tube was interfaced to a PDP-12 computer. All other spectral measurements were made using a Cary 14.

Electron-spin resonance measurements were made with a Varian E-9 ESR spectrometer. The peak-to-peak amplitude of the quartet due to Cu(II) (at a frequency of 4.430 GHz and a power of 2.5 mW) was used as a measure of the Cu(II) concentration. A linear relationship, ±6%, was obtained for each of the four peak heights vs. the concentration of copper up to the saturation limit of copper. All ESR experiments were run at room temperature.

The catalytic decay of hypochlorite also was monitored by measuring the volume of O_2 gas evolved. All measurements were made at atmospheric pressure. The number of moles of oxygen was calculated with appropriate correction for the temperature, the overall pressure, and the vapor pressure of water.

Chloride concentration was monitored with a chloride specific electrode (Orion Model 94-17A) and a saturated KCl–calomel reference electrode in contact with the test solution via a saturated sodium nitrate–agar bridge.

All measurements were made at 25.0 °C unless otherwise noted.

Results

Copper(II) Species in NaOH Solution. Evidence for Low Concentrations of $Cu_2(OH)_6^{2-}$. In the strongly basic media used in this work, copper(II) exists as a mixture of soluble anionic hydroxide species[8,29] with $Cu(OH)_4^{2-}$ generally predominating. The solubility of copper in basic solution has been investigated by McDowell and Johnston.[8] The solubility limits they report have been exceeded in a few solutions used in this work. However, these solutions have always been freshly prepared and have been quite stable in the absence of any CuO precipitate.

The ratio of $Cu(OH)_4^{2-}$ to $Cu(OH)_3^-$ has been calculated up to 2.0 M NaOH.[29] Above this level of base, Cu(II) is overwhelmingly $Cu(OH)_4^{2-}$ and its absorbance at 650 nm in 8.0 M NaOH shows no deviation from a linear Beer–Lambert relationship (ϵ 34.6 M^{-1} cm^{-1}) up to 0.03 M Cu(II). The same solution has an absorbance shoulder at 310–330 nm which does not depend upon [Cu(II)] but rather has a $[Cu(II)]^2$ dependence as shown in Figure 1.

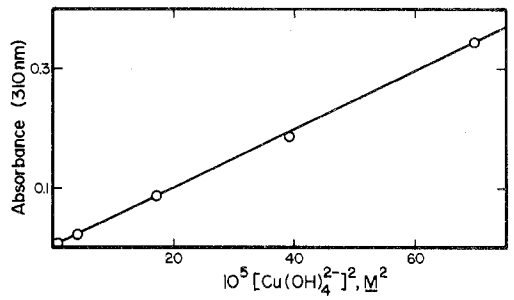

Figure 1. Spectrophotometric evidence for a dimeric copper(II) hydroxide complex in 8.0 M NaOH (25 °C; λ 310 nm; path length 5 cm).

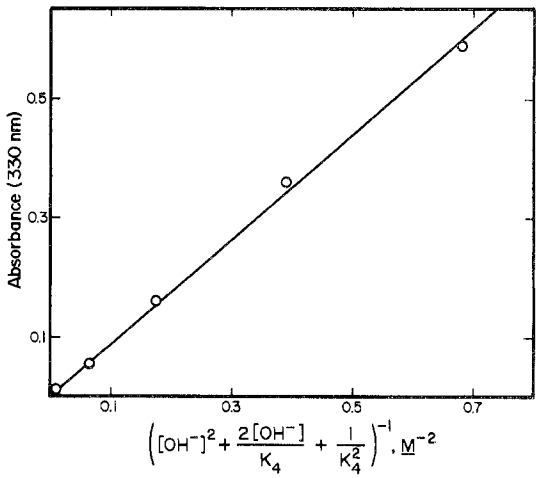

Figure 2. Hydroxide dependence of the absorption band of the copper(II) dimer indicating $Cu_2(OH)_6^{2-}$ is in equilibrium with $Cu(OH)_4^{2-}$ and $Cu(OH)_3^-$ ([Cu(II)] = 3.13 × 10^{-3} M, λ 330 nm, 25 °C, 5.0-cm path length).

The absorbance of this shoulder also was observed to vary with the inverse square of the hydroxide ion concentration. If the equilibrium governing the dimer formation is

$$2Cu(OH)_4^{2-} \overset{K_D}{\rightleftharpoons} Cu_2(OH)_6^{2-} + 2OH^- \quad (3)$$

and if $[Cu_2(OH)_6^{2-}]$ is much less than $[Cu(II)]_{total}$, then

$$[Cu_2(OH)_6^{2-}] = K_D[Cu(II)]^2_{total}\left(\frac{1}{[OH^-]^2+\frac{2[OH^-]}{K_4}+\left(\frac{1}{K_4}\right)^2}\right) \quad (4)$$

where K_4 is the concentration equilibrium constant for

$$Cu(OH)_3^- + OH^- \rightleftarrows Cu(OH)_4^{2-} \quad (5)$$

Absorbances at 330 nm, obtained by a variation of hydroxide ion over the range 1.2–9.7 M at constant [Cu(II)], are plotted vs. $([OH^-]^2 + 2[OH^-]/K_4 + (1/K_4)^2)^{-1}$ in Figure 2. The data in Figures 1 and 2 confirm the stoichiometry of the Cu(II) dimer to be $Cu_2(OH)_6^{2-}$. Neither the ESR signal nor the Beer–Lambert relationship at 650 nm of the Cu(II) monomer deviates from linearity. If it is assumed, therefore, that the dimeric species represents less than 5% of the total Cu(II) in solution, then the molar absorptivity of $Cu_2(OH)_6^{2-}$ at 310 nm must be greater than 520 M^{-1} cm^{-1}.

Stoichiometry and Kinetics of Hypohalite Decomposition. When Cu(II) is mixed with a large excess of OCl^- or OBr^-

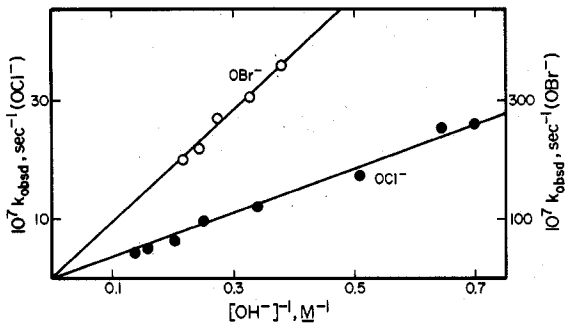

Figure 3. Resolution of the hydroxide dependence of the decomposition of the hypohalites showing the inverse hydroxide relationship for both monomeric and dimeric pathways (25 °C, [Cu(II)] = 1.98×10^{-4} M for OCl^-, [Cu(II)] = 4.20×10^{-4} M for OBr^-).

Table I. Effect of [Cu(II)] on the Observed Rate of Decomposition of Hypohalite Ion (25 °C)

OCl^- [a]		OBr^- [b]	
10^4[Cu(II)], M	$10^6 k_{obsd}$, s^{-1}	10^4[Cu(II)], M	$10^6 k_{obsd}$, s^{-1}
0.660	0.260	1.4	5.0
1.98	1.35	2.8	15.8
3.63	3.50	4.2	30.0
5.28	6.70	5.6	55.0
6.60	9.48		
7.92	13.4		

[a] $[OH^-] = 2.96$ M; $[OCl^-]_0 = 0.174$ M. [b] $[OH^-] = 3.00$ M; $[OBr^-]_0 = 0.200$ M.

in strong alkali, a deep yellow color develops in less than 30 s. Oxygen evolution begins a few seconds thereafter. Over a period of hours the concentration of hypohalite decreases as oxygen evolution continues. The expected 2:1 stoichiometry (eq 2) of OCl^- decomposed to O_2 formed was confirmed to within ±2% by measuring the oxygen gas formed from the copper-catalyzed decomposition.

The total amount of chloride produced in the catalyzed decomposition of hypochlorite was determined by decomposing OCl^- in solutions of 2 or 4 M NaOH with varying [Cu(II)] from 1.65×10^{-3} M to 9.9×10^{-3} M. Two weeks was allowed for the decomposition to take place. The identical concentration of OCl^-, without Cu(II), decomposed by Na_2SO_3, was used as the standard. All solutions were diluted into 0.57 M phosphate buffer and brought to pH 7.09 ± 0.02 with perchloric acid. The value of 0.84 ± 0.01 M chloride was obtained for the standard and 0.78 ± 0.03 M chloride for the average of six copper-catalyzed decompositions.

The kinetics of the decomposition of OCl^- were followed by the volume of O_2 formed and by the spectral changes in the solution. Solutions of 1.65×10^{-3} M Cu(II) and 1.90 M NaOH were used to compare the observed first-order rate constants. For the oxygen study, a k_{obsd} of $(5.88 \pm 0.17) \times 10^{-5}$ s^{-1} was obtained from the rate expression $d[O_2]/dt = k_{obsd}([O_2]_\infty - [O_2])$. The spectral study resulted in a k_{obsd} of $(5.68 \pm 0.07) \times 10^{-5}$ s^{-1} which was obtained from the rate expression $-d[OCl^-]/dt = k_{obsd}[OCl^-]$.

The effects of varying the concentrations of OH^-, Cu(II), and halide ions were observed spectrally for the rate of decomposition of both OCl^- and the analogous OBr^- reactions. Figure 3 shows an inverse-first-order hydroxide dependence for the decomposition of both hypohalites. Table I presents the effect of changing the concentration of Cu(II). The nonlinear behavior indicates the presence of the greater than first-order terms in copper as had been observed by Prokopcikas[6] and Sakharov.[7] Chloride concentration was varied up to 1.0 M and showed no effect on the decomposition of OCl^-. The effect of bromide concentration on the OBr^- decomposition will be presented later.

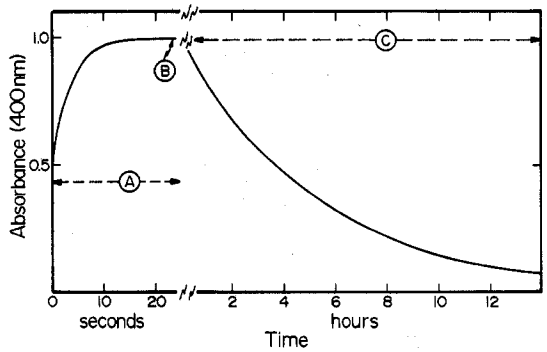

Figure 4. Absorbance behavior at 400 nm of a mixture of 3.0 M NaOH, 1.65×10^{-3} M Cu(II), and 0.2 M OCl^- at 25 °C.

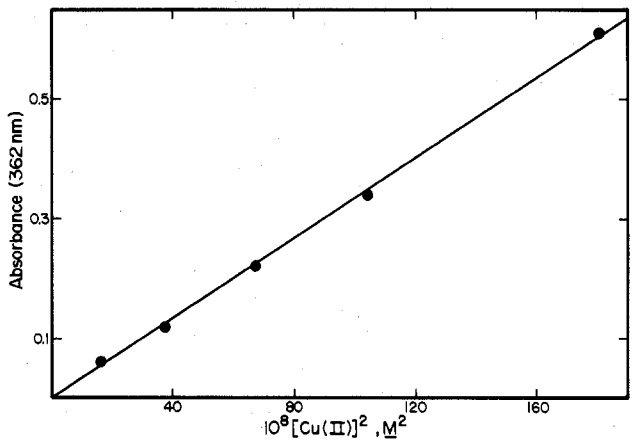

Figure 5. The $[Cu(II)]^2$ dependence on the absorbance of the yellow intermediate at 362 nm indicating the involvement of two Cu(II) centers (25 °C, $[OCl^-] = 0.217$ M, $[OH^-] = 2.5$ M, slope 3.39×10^5 M^{-2}).

Table II. Dependence of the Absorbance of B_{max} on OCl^- and OH^- Concentrations[a]

$[OCl^-]$, M	$[OH^-]$, M	Abs (362 nm)	$[OCl^-]$, M	$[OH^-]$, M	Abs (362 nm)
0.043	1.88	0.035	0.217	1.13	0.355
0.087	1.88	0.069	0.217	1.50	0.252
0.130	1.88	0.119	0.217	2.62	0.134
0.174	1.88	0.158	0.217	3.38	0.111
0.217	1.88	0.196	0.217	4.00	0.091

[a] $[Cu(II)] = 2.05 \times 10^{-3}$ M, path length 1.0 mm, 25 °C.

Formation of the Yellow Species. The change in absorbance at 400 nm after mixing Cu(II) and OCl^- is presented in Figure 4. The same type of behavior is observed from 330 to 450 nm. Section C in Figure 4 corresponds to the long decomposition reaction presented above. Section A is the increase in absorbance due to the formation of the yellow species. Point B is the maximum absorbance of the solution and the maximum concentration of the intermediate. A number of other ligands (thiocyanate, cyanate, acetate, ammonia, hypoiodite, chloride, bromide, and iodide) under similar conditions ($[Cu(II)] = 6.60 \times 10^{-4}$ M, $[OH^-] = 2.4$ M, and [ligand] = 0.25 M) show no observable chemical reaction or spectral change at wavelengths greater than 260 nm.

The maximum absorbance at 362 nm due to the yellow species (B_{max}), formed with OCl^-, was monitored on a Cary 16 while varying the concentration of the reactants present in solution as shown in Table II and Figure 5. The absorbance due to B_{max} has a first-power dependence in OCl^- and an inverse-first-power dependence in OH^-. The absorbance of the yellow species is seen to vary linearly with $[Cu(II)]^2$.

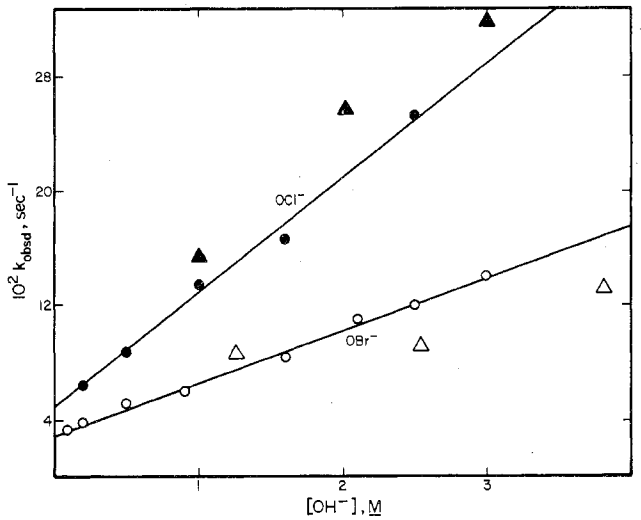

Figure 6. Hydroxide dependence of the decay of the Cu(III) intermediate formed by oxidation using OCl^- and OBr^- (25 °C). OCl^-: ●, dilution experiments; ▲, stopped-flow experiments. OBr^-: ○, dilution experiments; △, stopped-flow experiments.

The broad absorption band centered around 640 nm due to $Cu(OH)_4^{2-}$ also was monitored in the time regime of the maximum absorbance at 362 nm. Dual 1-cm compartment difference cells (2-cm total path length) were used. Solutions of Cu(II) and OCl^-, each with identical OH^- concentrations, were placed in separate compartments of the reference cell. More of the same solutions were mixed equally and placed in both compartments of the sample cell. Under no conditions could any change be seen in the absorbance at 640 nm. The ESR spectrum of Cu(II), which yielded a quartet of peaks ([NaOH] = 1–8 M), failed to show any change upon addition of OCl^- up to 0.23 M within the precision of the instrument. Hence, there appears to be no appreciable loss of Cu(II) during the reaction.

The development of the yellow color (region A of Figure 4) was monitored by the stopped-flow method for both OCl^- and OBr^-. The increase in yellow color exhibits a pseudo-first-order behavior in that a plot of ln $(B_{max} - B)$ vs. time gives a linear relationship despite the observation that the concentration of Cu(II) does not appear to change appreciably. Also, the OH^- and OX^- species are in great excess and their concentrations could not change appreciably even if all the copper were converted to the yellow species.

Analysis of this first-order behavior shows it to be independent of [Cu(II)] or [OX^-]. It is, however, dependent on [OH^-] as shown in Figure 6. These data are somewhat scattered due to the eventual formation of oxygen bubbles in the observation cell of the stopped-flow apparatus. The peculiar kinetic dependences observed for the appearance of the yellow species are discussed later.

Direct measurement of the absorption spectrum of the yellow species is difficult to obtain under conditions necessary to form a substantial absorbance because of the overlapping strong absorbance of the hypohalites and O_2 evolution. Nevertheless, a corrected spectrum was obtained directly from 330 to 400 nm for the intermediate formed with OCl^- and exhibited a λ_{max} at 362 nm. The analogous experiment with OBr^- was prevented by the absorbance maximum of OBr^- at 329 nm.

Rapid-Dilution Experiments. A rapid 20–30-fold dilution of solutions containing the yellow species has provided a series of key experiments which have permitted the characterization of this species as a Cu(III) complex. First of all, the dilution experiment makes it clear that the yellow species B is not a copper(II) hypohalite complex. A Cu(II) complex would be

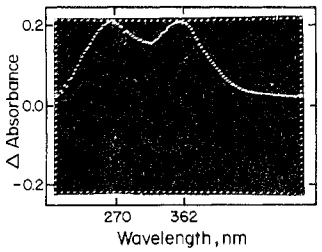

Figure 7. Absorption spectrum of the Cu(III) intermediate (path length 1 cm, 25 °C).

expected to dissociate instantaneously upon dilution in accord with the general kinetic behavior of Cu(II) and the specific substitution behavior known for $Cu(OH)_4^{2-}$ and $Cu(OH)_3^-$.[29] Secondly, the dilution experiments allow the true decay of the species B to be measured independently of the formation of B since this formation is not appreciable in the dilute solutions.

The decay of B was followed by rapidly (<2 s) diluting a small volume (~0.1 mL) of a reacting solution containing hypohalite, Cu(II), and OH^- into 2 or 3 mL of base. The decay of the yellow species exhibited first-order behavior overall. The kinetic dependences were the same as those dependences from the stopped-flow studies following the increase of the yellow species. The decay of B was also observed by dilution into solutions containing NaOH and the hypohalite not used to form the intermediate. No dependence on the hypohalite in the diluent was seen. Plots of k_{obsd} vs. [OH^-] for the decay of the intermediate formed from OCl^- and OBr^- are shown in Figure 6.

This dilution method also was used to obtain a complete spectrum of the intermediate formed with OCl^- or OBr^- using the vidicon rapid-scanning spectrophotometer. After dilution, two sets of eight spectra (one spectrum every 10 ms) were recorded. One set was recorded immediately, and the other set after the intermediate had decayed. The spectrum of the intermediate alone was obtained by subtracting the average of the second group of eight spectra from the average of the first group of eight spectra. The spectrum of the intermediate formed by reacting Cu(II) with OCl^- or OBr^- is shown in Figure 7.

Effect of Bromide on the Reactions of Hypobromite. The concentration of chloride does not affect any reactions with OCl^- or OBr^-. However, the concentration of bromide can have an effect on the reactions with OBr^-.

The overall decomposition of OBr^- is slowed by increased bromide concentration. Solutions of 1.04×10^{-3} M Cu(II), 2.0 M NaOH, and initially 0.086 M OBr^- plus either 1.10 M Br^- or 2.30 M Br^- were allowed to decay. The observed first-order rate constants obtained were 1.04×10^{-4} s^{-1} for 2.30 M Br^- and 2.26×10^{-4} s^{-1} for the case of 1.10 M Br^-. A k_{obsd} of 2.45×10^{-4} s^{-1} is expected for a solution initially free of bromide.

The dilution experiments also are affected by bromide. Solutions of OBr^-, OH^-, and Cu(II) which had formed species B were diluted into solutions of varying bromide ion concentrations. The [OH^-] was kept at low levels in order to minimize the hydroxide-accelerated decay presented previously. Figure 8 shows that the decay of B has a first-order dependence in bromide concentration. At 0.54 M bromide, the hydroxide concentration was varied from 0.094 to 2.05 M. In this range, hydroxide did not affect the bromide-accelerated decay of B. It is important to note that the dilution decay reactions, under all conditions, remained first order.

Solutions of Cu(II), OH^-, and OCl^- which had formed species B were also diluted into solutions containing Br^-. Qualitatively, bromide accelerated the decay of B in this case also, but the interference of the formation of OBr^- from the reaction of HOCl with Br^- does not permit quantitative

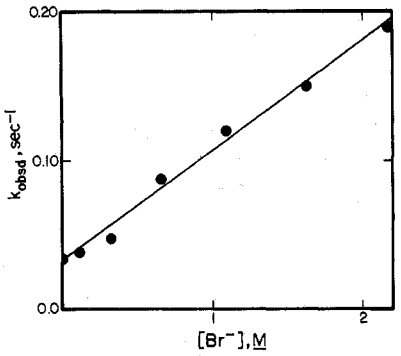

Figure 8. Bromide dependence on the rate constant for the reduction of the Cu(III) intermediate by Br^- to give OBr^- and Cu(II) in 0.094, M NaOH at 25 °C.

analysis of this bromide-accelerated rate.

Discussion

General Kinetic Behavior. At wavelengths less than 425 nm, the absorbance of a solution containing OCl^- or OBr^-, Cu(II), and NaOH is due to the sum of the hypohalite contribution and that of an intermediate species. The absorbance–time relationship of these solutions has been shown in Figure 4. A similar relationship is observed at longer wavelengths where only Cu(II) and the intermediate contribute to the absorbance.

This type of kinetic behavior is most simply described by the general mechanism for a two-step consecutive reaction shown in eq 6, where the absorbance of the intermediate

$$A \xrightarrow{k_{AB}} B \xrightarrow{k_{BC}} C \tag{6}$$

species B is monitored. The concentrations of the individual species are given by eq 7–9.

$$[A] = [A]_0 e^{-k_{AB}t} \tag{7}$$

$$[B] = \frac{[A]_0 k_{AB}}{k_{BC} - k_{AB}}(e^{-k_{AB}t} - e^{-k_{BC}t}) \tag{8}$$

$$[C] = \frac{[A]_0}{k_{BC} - k_{AB}}((k_{BC}(1 - e^{-k_{AB}t}) - k_{AB}(1 - e^{-k_{BC}t})) \tag{9}$$

For this general mechanism, two sets of conditions could explain the type of absorbance–time profile observed for B:[30] case I, $k_{AB} >> k_{BC}$ and the absorptivity of B is not much greater than that of A; case II, $k_{BC} >> k_{AB}$ and the absorptivity of B is large compared to that of A. Thus, case I represents the situation in which a substantial amount of the intermediate is formed compared with the initial amount of reactant and then slowly decays. This was the behavior postulated by Lister[2] in his experiments in which he concluded that all the copper was converted to the intermediate. On the other hand in case II, only a small amount of highly absorbing intermediate exists at any time since its decay is rapid in comparison to its formation.

Several points may be offered against the choice of case I to explain the observed copper-catalyzed system. (1) Since the hypohalite is in large excess over copper (approximately 100-fold initially), the slow decay would be zero order in case I, but, experimentally, this is not the case. (2) The kinetic and absorbance dependences do not fit any logical pattern under case I. (3) The spectral characteristics in the 500–700-nm range due to $Cu^{II}(OH)_4^{2-}$ and the ESR signal due to Cu(II) are retained after addition of the hypochlorite.

On the other hand, the observed behavior can be explained adequately by case II. When $k_{BC} >> k_{AB}$ and the value of t is large, eq 8 may be written as

$$[B] = \frac{[A]_0 k_{AB}}{k_{BC}}(e^{-k_{AB}t}) \tag{10}$$

or

$$\ln([B] - [B]_\infty) = -k_{AB}t + \ln\left(\frac{[A]_0 k_{AB}}{k_{BC}}\right) \tag{11}$$

In terms of the formation of C (C corresponds to oxygen gas and halide ion) eq 9 reduces to eq 12 at large values of time.

$$[C] = [A]_0(1 - e^{-k_{AB}t}) \tag{12}$$

The stoichiometry of the reaction leads to eq 13. Thus, the

$$\ln([O_2]_\infty - [O_2]) = -k_{AB}t + \ln\left(\frac{[A]}{2}\right) \tag{13}$$

slow decomposition of B and OX^- and the associated formation of O_2 are all governed by k_{AB}, the rate constant for the *formation of the intermediate* (eq 7, 10–13). The general agreement between the kinetic order dependences of k_{AB} and the absorbance dependences of the intermediate in [Cu(II)], $[OCl^-]$, and $[OH^-]$ gives additional support to this interpretation. Since $d[C]/dt = -d[A]/dt$ when the concentration of B is small, k_{AB} should be obtainable following the change in concentration of X^-, OX^-, O_2, or B at long times. Indeed the observed rate constants of $(5.88 \pm 0.17) \times 10^{-5}$ s^{-1}, following O_2 formation, and of $(5.68 \pm 0.07) \times 10^{-5}$ s^{-1}, following the spectrophotometric long-term decomposition of B and OX^- under the same conditions, do agree.

For the situation where t is small, eq 8 can be written

$$\ln([B]_{max} - [B]) = -k_{BC}t + \ln\left(\frac{[A]_0 k_{AB}}{k_{BC}}\right) \tag{14}$$

where $[B]_{max}$ represents the maximum concentration of B produced. Thus the rate constants obtained from the stopped-flow experiments which *appear to be* associated with the formation of the intermediate are *actually controlled by the kinetics of the decomposition of the intermediate.* The lack of any kinetic dependence for both Cu(II) and hypohalite are consistent with a pseudo-first-order decay process while the hydroxide, present in large excess, catalyzes the decomposition.

A further test of this mechanism is afforded by the dilution experiments. Since the observed rate constants for the formation of the intermediate is proportional to the concentration of the hypohalite and to mixed orders in [Cu(II)], rapid dilution of a small amount of a reacting mixture of Cu(II) and OX^- by a factor of 10 (at constant $[OH^-]$) should decrease the rate of formation of the intermediate by a factor of approximately 10^3, effectively halting the formation process. Thus, it is possible to follow the decay of the intermediate directly. The agreement of the results from measuring k_{BC} by dilution compare well with the stopped-flow data (Figure 6).

The assumption that only a small amount of the Cu(II) present is converted to the intermediate may also be tested by calculating the concentration of the intermediate using observed rate constants under specified conditions. The value of $[B]_{max}$ is given by eq 15 (see Appendix), where $[A]_0$

$$[B]_{max} = [A]_0 k_{AB}/k_{BC} \tag{15}$$

represents the initial hypohalite concentration and the condition of $k_{BC} >> k_{AB}$ is invoked. Correspondingly, the time at which this point is reached, t_{max}, may be estimated by eq 16 (see

$$t_{max} \approx \frac{\ln(k_{BC}/k_{AB})}{k_{BC}} \tag{16}$$

Table III. Range of $[B]_{max}$ and t_{max} from Experimental Conditions Used in This Work for OCl^- [a]

$[OH^-]$, M	[Cu(II)], M	$[B]_{max}$, M	t_{max}, s
3.0	1.0×10^{-3}	$\sim 1.4 \times 10^{-5}$	~33
8.0	4.0×10^{-4}	$\sim 8.4 \times 10^{-7}$	~17

[a] $[OCl^-] = 0.40$ M, 25 °C.

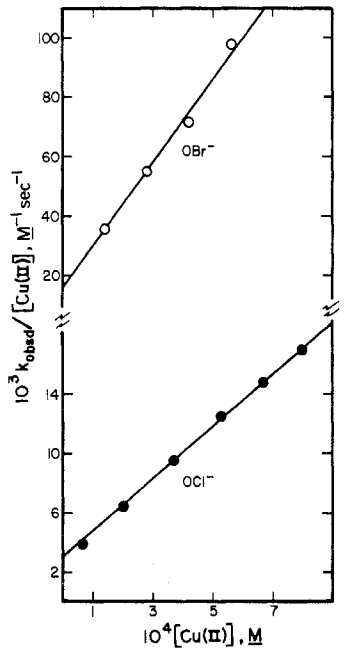

Figure 9. Resolution of the Cu(II) dependence for the decay of OCl^- and OBr^- which shows the Cu(II) dimeric (slope) and monomeric (intercept) pathways in 3.0 M NaOH at 25 °C: ●, OCl^-; ○, OBr^-.

Appendix). Calculations of $[B]_{max}$ and t_{max} are given in Table III for experimental conditions which produced the highest and lowest values of $[B]_{max}$ and t_{max} observed in this work. The low values of $[B]_{max}$ agree with the constant Cu(II) signal during the reaction as seen spectrally and by ESR. Precise experimental values of t_{max} could not be obtained from the stopped-flow studies because of the formation of oxygen bubbles at times greater than 20–25 s. It might also be noted that in a highly supersaturated solution of Cu(II) (e.g., 3×10^{-3} M Cu(II), 1.00 M NaOH) mixed with 0.4 M OCl^-, as much as 50% of the copper present could be converted to the intermediate. This should clearly give a change in the Cu(II) absorbance. Unfortunately, under these conditions the nucleation process is fast and copper oxide precipitates. (It may be noted that this is essentially the method for preparing sodium dioxocuprate(III).[5])

Resolution of Rate Constants. The kinetic data for the slow absorbance loss of both hypohalites exhibit a mixed-order dependence on [Cu(II)] as shown in Table I. By dividing the observed rate constants by the copper concentration (at constant hydroxide ion concentration), and by plotting that quotient vs. [Cu(II)], a linear relationship is obtained as seen in Figure 9. For OCl^-, the slope is (17.5 ± 0.5) M^{-2} s^{-1} and the intercept is (3.1 ± 0.3) × 10^{-3} M^{-1} s^{-1}. For OBr^-, the slope is (140 ± 10) M^{-2} s^{-1} and the intercept is (1.5 ± 0.4) × 10^{-2} M^{-1} s^{-1}.

The general relationship implies that two pathways exist. One pathway corresponds to a first-order dependence in [Cu(II)] as proposed by Lister.[2] The other pathway shows a second-order dependence in copper as proposed by Prokopcikas.[6] Neither Lister nor Prokopcikas worked over a large enough range to observe both pathways. The 1.7 order dependence reported for Cu(II) in the catalysis of OBr^- decay[7] can thus be explained as data taken in the region where the squared dependence predominates but does not totally control the reaction.

Table IV. Resolved Rate Constants (25 °C)

		OCl^-	OBr^-
k_{AB}	k_1, s^{-1}	(9.2 ± 0.8) × 10^{-3}	(44 ± 1) × 10^{-3}
	k_2, M^{-1} s^{-1}	51.8 ± 0.2	410 ± 20
k_{BA}	k_{-2}, M^{-1} s^{-1}	Not determined	0.073 ± 0.003
k_{BC}	$k_{BC}^{OH^-}$, M^{-1} s^{-1}	0.080 ± 0.004	0.037 ± 0.001
	$k_{BC}^{H_2O}$, s^{-1}	0.049 ± 0.006	0.030 ± 0.002

The hydroxide dependence is resolved as a simple inverse order as shown in Figure 3. The slope for OCl^- is (3.9 ± 0.3) × 10^{-6} M s^{-1} and the slope for OBr^- is (9.3 ± 0.7) × 10^{-4} M s^{-1}. The intercepts of both plots are not significantly different from zero indicating that both copper pathways follow the same hydroxide ion concentration dependence.

From this, the dependence of k_{AB}(obsd) can be written

$$k_{AB}(\text{obsd}) = \frac{k_1[\text{Cu(II)}]}{[OH^-]} + \frac{k_2[\text{Cu(II)}]^2}{[OH^-]} \quad (17)$$

where k_1 and k_2 are the rate constants for the first- and second-order copper pathways, respectively. The resolved rate constants are given in Table IV.

The resolution of k_{BC} is presented in Figure 6. Decomposition of the intermediate was affected only by $[OH^-]$ and, in case of OBr^-, by high bromide concentrations. However, high bromide ion concentration also lowers the amount of intermediate formed and slows the overall decay of OBr^- indicating that this condition is really a special case where the k_{AB} step has some reversibility. Without this reversibility, k_{BC}(obsd) can be written

$$k_{BC}(\text{obsd}) = k_{BC}^{OH}[OH^-] + k_{BC}^{H_2O} \quad (18)$$

where k_{BC}^{OH} is the slope of each line in Figure 6 and $k_{BC}^{H_2O}$ (independent of OH^-) is the intercept. These calculated constants are presented in Table IV.

The first step, k_{AB}, in the decomposition of OBr^- shows significant reversibility in the presence of high concentrations of bromide ion. The general mechanism of OBr^- decay in high bromide ion concentration is shown in eq 19, where k_{BA} and

$$A \underset{k_{BA}}{\overset{k_{AB}}{\rightleftharpoons}} B \xrightarrow{k_{BC}} C \quad (19)$$

k_{BC} have become comparable. The contribution of k_{BC} can be minimized at low hydroxide ion concentration. Figure 8 presents the variation of k_{obsd} with bromide ion concentration at constant hydroxide ion concentration. The intercept is k_{BC} for OBr^- at 0.094 M NaOH. Since the k_{BA} path is independent of hydroxide ion concentration and is only dependent on bromide ion concentration, the expression for k_{BA}(obsd) is

$$k_{BA}(\text{obsd}) = k_{-2}[Br^-] \quad (20)$$

where k_{-2} (the slope of Figure 8) is 0.073 M^{-1} s^{-1} (Table IV).

Nature of the Intermediate. Lister[2] described the yellow species produced by hypochlorite, Cu(II), and NaOH as the trivalent copper species $Cu(OH)_4^-$. If the intermediate was $Cu(OH)_3(OCl)^{2-}$, as Magee and Wood[5] suggested, then hypoiodite, a stronger base than OCl^- or OBr^-, should yield a similar complex with Cu(II). Experimentally, $Cu(OH)_3(OI)^{2-}$ cannot be detected. This implies that the intermediate is not a Cu(II) species. Furthermore, the kinetic behavior of

the intermediate shows that the species is not a Cu(II) complex.

If the yellow species was a product of any equilibrium involving Cu(II), reestablishment of that equilibrium would take place within the mixing time, as does the equilibrium of other substitution reactions of Cu(II) in NaOH solutions. Values of k_{BC} and k_{BA} are many orders of magnitude slower than would be possible for any Cu(II) complex. On the other hand, the decay of the intermediate to O_2 is quite comparable to the decay rate constant of copper(III) tetraglycine in 1 M NaOH which is approximately 0.3 s^{-1}.[31]

The spectrum of the intermediate adds further credence to the presence of a Cu(III) species. The absorbance maxima of 362 ± 2 and 270 ± 2 nm (Figure 7) are remarkably similar to those for copper(III) tetraglycine (365 ± 2 and 250 ± 2 nm) and copper(III) triglycine (385 ± 2 and 262 ± 2 nm).[32] Also, Prokopcikas and Butkevicius[33] reported an absorbance maximum at 360 ± 5 nm for the product formed from electrochemical oxidation of copper in basic solution. In order to calculate the molar absorptivity of the intermediate, eq 15 can be rearranged to

$$\frac{A_{B_{max}}}{\epsilon_B} = \frac{k_2[OCl^-]_0[Cu(II)]^2}{(k_{BC}^{OH}[OH^-] + k_{BC}^{H_2O})[OH^-]} \tag{21}$$

or

$$\epsilon_B = \frac{(k_{BC}^{OH}[OH^-] + k_{BC}^{H_2O})[OH^-]}{k_2[OCl^-]_0}\left(\frac{A_{B_{max}}}{[Cu(II)]^2}\right) \tag{22}$$

where ϵ_B is the molar absorptivity of B, $A_{B_{max}}/[Cu(II)]^2$ is the slope of the absorbance of B_{max} as a function of $[Cu(II)]^2$ (Figure 5), and $[OH^-]$ and $[OCl^-]_0$ are the concentrations at which that slope was obtained. From this, ϵ_B is ~18 800 M^{-1} cm^{-1}. This value of 9400 M^{-1} cm^{-1} per Cu(III) is comparable with the molar absorptivities calculated for the copper(III) peptide complexes.[16-18]

Although the oxidation state of the copper proposed by Lister[2] is confirmed, the empirical formula of the Cu(III) species requires further consideration. The condition where the initial step in the OBr^- decay is reversible affords the most useful information. Since the absorbance of the intermediate at its maximum concentration is kinetically controlled and only has a squared dependence in [Cu(II)], this reaction path will be treated first.

The equilibrium of the reactants and intermediate(s) is, of course, the quotient of the forward and reverse rates. The forward and reverse rates are governed by

$$r_f = \frac{k_2[Cu(OH)_4^{2-}]^2[OBr^-]}{[OH^-]} \tag{23}$$

and

$$r_r = k_{-2}[Br^-][B] \tag{24}$$

Note that the decay of the intermediate B is *first order* when $[Br^-]$ is held constant. Therefore, the equilibrium may be written

$$2Cu(OH)_4^{2-} + OBr^- \overset{K_2}{\rightleftharpoons} Br^- + OH^- + B \tag{25}$$

This requires the formula of the intermediate to be $Cu^{III}_2(O)(OH)_7^{3-}$ subject to any equivalent loss or gain of H_2O molecules to vary the ratio of oxides vs. hydroxides. From Figures 1 and 2, $Cu^{II}_2(OH)_6^{2-}$ was shown to exist in solution. This molecule would only have to add one hydroxide before adding OBr^- in order to be considered the reactive species. The dimeric structure is also supported by the low reduction potential of the Cu(III) moiety. The value of K_2 for eq 25 as written is equal to 5600. Therefore, $E°$ for eq 26 in 1 M

$$Cu^{III}_2(O)(OH)_7^{3-} + H_2O + 2e^- \rightarrow 2Cu^{II}(OH)_4^{2-} + OH^- \tag{26}$$

NaOH is 0.82 V vs. NHE. This $E°$ value corresponds to values found for copper(III) peptide complexes. However, the $E°$ value in eq 26 is much lower than would be predicted for Cu(III) with four OH^- ions. This suggests that the presence of coordinated oxide(s) may be lowering the potential.

Other dinuclear Cu(III) species have been postulated. The solid $Ba(CuO_2)_2$[4] has been proposed to be an oxide-bridged dimer. Jameson and Blackburn[34,35] have proposed dimeric Cu(II)–Cu(III) electron transfers in the autoxidation of ascorbic acid with O_2. They have explained their observations via a very small concentration of a dinuclear copper(II)–ascorbic acid complex reacting with O_2 to oxidize the two copper(II) atoms to a Cu^{III}_2–ascorbic acid intermediate. Rozovskii, Misyavichyus, and Prokopchik[36] have also observed kinetic evidence for dimer formation in the decomposition of copper(III) tellurate complexes in alkaline solution.

Treatment of the forward path, which is first order in copper, is intriguing. If a Cu(III) monomer is postulated as an intermediate, the electrons being transferred cannot be accounted for via an equilibrium similar to eq 25 while maintaining the first-order dependence in copper for the k_{-2} process (eq 24). Similarly, the monomer path cannot proceed to form a dimer by eq 27 and 28 because this would require

$$Cu^{II} + OBr^- \rightleftarrows Cu^{IV} + Br^- \tag{27}$$

$$Cu^{IV} + Cu^{II} \rightleftarrows Cu^{III}_2 \tag{28}$$

a reverse rate dependence as shown in eq 29; however, the

$$\frac{-d[Cu^{III}_2]}{dt} = \frac{k[Cu^{III}_2][Br^-]}{k'[Cu^{II}] + k''[Br^-]} \tag{29}$$

inverse copper dependence is not observed.

However, certain inferences can be drawn concerning the mechanism of the monomeric pathway. If reactions are limited to two-electron transfers, the observed kinetic dependences would be satisfied in at least two cases. (1) A $Cu^{II}(OH)_3(OCl)^{2-}$ complex is produced which then forms a $Cu^{II}(O_2)(OH)_2^{2-}$ peroxo species intramolecularly. This species could then react rapidly with another hypohalite ion to produce O_2. (2) The $Cu(OH)_3^-$ complex might react with OX^- to form a Cu(IV) intermediate. This would also be very reactive toward solvent or OX^-.

The discussion to this point would conclude that species B is identical for oxidation with both OCl^- and OBr^-. However, the data in Figure 6 point out that the decay of the yellow species is not the same when it is produced in the solutions with OCl^- in comparison to the solutions with OBr^-. The differences are small but reproducible (ratios of k_{BC} of OCl^- to OBr^- vary from 1.2 to 2.0 over the range of 0–3 M NaOH). Microscopic reversibility does not permit an OBr^- or Br^- to be involved in the intermediate subsequent to the hypobromite oxidation of the Cu(II) species. Because of the lack of reversibility in the OCl^-/Cl^- system, the analogous statement cannot be made as strongly for OCl^-. However, since OBr^- is a stronger base than OCl^-, it is unlikely that OCl^- could fully convert $Cu^{III}_2(O)(OH)_7^{3-}$ to a copper(III) hypochlorite complex. This would be necessary in order to include OCl^- in the intermediate without including an OCl^- dependence in the decay kinetics of the intermediate. Chloride ion has been shown to have no effect in the OCl^- reaction. Furthermore, within our ability to measure, the spectrum of the intermediate is the same for both hypohalites. The reason for the difference in the decay rates in Figure 6 is not understood. Aside from these data, species B appears to be identical for both hypohalite reactions. It is of note that Jameson and Blackburn[35] also saw

Scheme I. Proposed Mechanism of the Copper-Catalyzed Decomposition of OCl^- and OBr^-

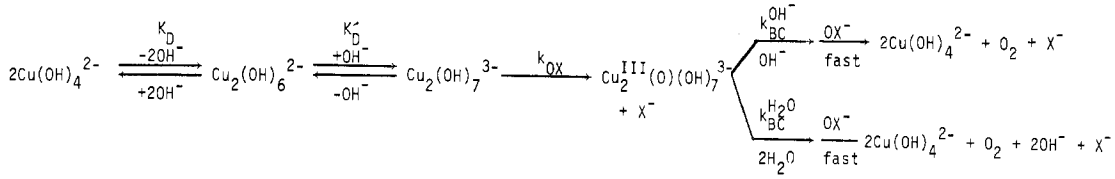

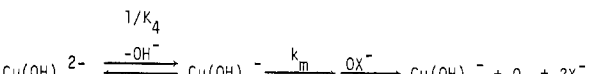

$$\frac{-d[OX^-]}{dt} = k_{OX}[Cu_2(OH)_7^{3-}][OX^-] + k_m[Cu(OH)_3^-][OX^-]$$

$$= \frac{k_{OX}K_D K_D'[Cu(OH)_4^{2-}]^2[OX^-]}{[OH^-]} + \frac{k_m K_4[Cu(OH)_4^{2-}][OX^-]}{[OH^-]}$$

$$K_D = \frac{[Cu_2(OH)_6^{2-}][OH^-]^2}{[Cu(OH)_4^{2-}]^2} \qquad K_D' = \frac{[Cu_2(OH)_7^{3-}]}{[Cu_2(OH)_6^{2-}][OH^-]} \qquad K_4 = \frac{[Cu(OH)_4^{2-}]}{[Cu(OH)_3^-][OH^-]}$$

H_2O

$$k_2 = k_{OX}K_D K_D' \qquad k_1 = k_m K_4 \qquad k_{BC} = k_{BC}^{OH^-}[OH^-] + k_{BC}^{H_2O}$$

Scheme II. Suggested Model of the Dimeric Pathway in the OBr^- Decomposition

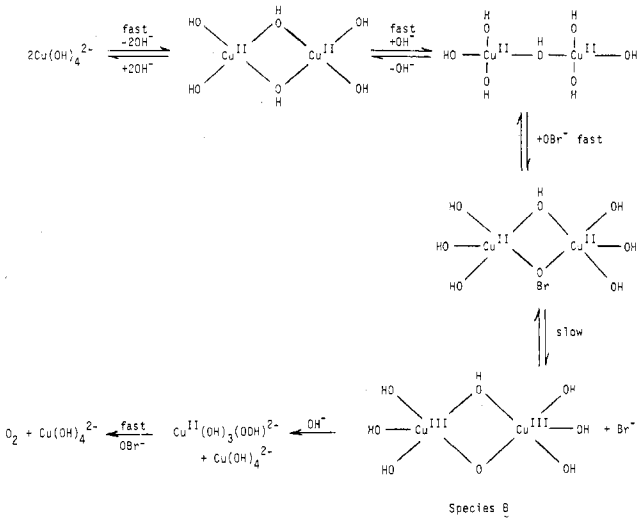

Species B

variations in the decay rates with the nature of the supporting electrolyte, but they did not observe a dependence on the concentration of those electrolytes.

Scheme I summarizes the mechanism of the copper-catalyzed decomposition of OCl^- and OBr^-. Scheme II presents a possible molecular model for the decomposition of OBr^- through the dimeric copper pathway.

Conclusions

A homogeneous solution of copper in a strongly basic medium is an effective catalyst for the conversion of OX^- to $^1/_2O_2 + X^-$, even at 10 μM copper concentrations and 25 °C. Two pathways for catalysis are observed. One follows an

$$A \xrightarrow{k_{AB}} B \xrightarrow{k_{BC}} C$$

mechanism where $k_{BC} >> k_{AB}$. This pathway exhibits a squared dependence on the total concentration of copper(II) present. The intermediate B has been shown to have the general formula $Cu^{III}_2(O)_n(OH)_{9-2n}^{3-} \pm nH_2O$ when OBr^- is used. Evidence for $Cu^{II}_2(OH)_6^{2-}$ in basic Cu(II) solutions suggests that this moiety is the reactive species in this pathway. The dimeric Cu(III) species exhibits two absorbance maxima in the ultraviolet and visible spectral regions with molar absorptivities of 9400 M^{-1} cm^{-1} per Cu(III). The reduction potential is only 0.82 V vs. NHE when reacting to give 2 equiv of $Cu(OH)_4^{2-}$ in 1 M NaOH. There are similarities between the copper(III) hydroxo dimer and the copper(III) peptide complexes in regard to the absorption spectra, $E°$ value, and rates of decay.

The hydroxide-bridged Cu(II) dimer appears to be an effective catalyst for these oxidations because of its ability to give up two electrons to form the Cu(III) dimer.

A monomeric Cu(II) pathway also is detected. Although effective catalytically, this is a slower pathway and only becomes significant at lower copper concentrations. This pathway does not produce an observable Cu(III) species.

Acknowledgment. This investigation was supported by the National Science Foundation under Grants CHE74-00043 and CHE75-15500.

Appendix

Derivation of $[B]_{max}$ and t_{max}

$$[B] = \frac{[A]_0 k_{AB}}{k_{BC} - k_{AB}}(e^{-k_{AB}t} - e^{-k_{BC}t})$$

$$\frac{d[B]}{dt} = \frac{[A]_0 k_{AB}}{k_{BC} - k_{AB}}(k_{BC}e^{-k_{BC}t} - k_{AB}e^{-k_{AB}t})$$

At $[B] = [B]_{max}$, $d[B]/dt \equiv 0$. Since $[A]_0 k_{AB}/(k_{BC} - k_{AB})$ cannot be zero

$$k_{BC}e^{-k_{BC}t_{max}} \equiv k_{AB}e^{-k_{AB}t_{max}} \qquad (A)$$

Solution of t_{max}

$$\frac{k_{BC}}{k_{AB}} = \frac{e^{-k_{AB}t_{max}}}{e^{-k_{BC}t_{max}}}$$

$$\frac{k_{BC}}{k_{AB}} = e^{(k_{BC} - k_{AB})t_{max}}$$

$$\ln (k_{BC}/k_{AB}) = (k_{BC} - k_{AB})t_{max}$$

$$t_{max} = \frac{\ln (k_{BC}/k_{AB})}{k_{BC} - k_{AB}}$$

Solution of $[B]_{max}$. Substituting eq A in the first equation

$$[B]_{max} = \frac{[A]_0 k_{AB}}{k_{BC} - k_{AB}} \left(\frac{k_{BC}}{k_{AB}} e^{-k_{BC}t_{max}} - e^{-k_{BC}t_{max}} \right)$$

$$= \frac{[A]_0 k_{AB}}{k_{BC} - k_{AB}} \left(\frac{k_{BC} - k_{AB}}{k_{AB}} e^{-k_{BC}t_{max}} \right)$$

$$[B]_{max} = [A]_0 e^{-k_{BC}t_{max}}$$

Substituting the equivalent expression for t_{max}

$$[B]_{max} = [A]_0 e^{(-k_{BC}/k_{BC} - k_{AB})(\ln (k_{BC}/k_{AB}))}$$

Under the restriction that $k_{BC} >> k_{AB}$

$$[B]_{max} = \frac{[A]_0 k_{AB}}{k_{BC}}$$

and

$$t_{max} = \frac{\ln (k_{BC}/k_{AB})}{k_{BC}}$$

Registry No. $Cu(OH)_2$, 20427-59-2; OCl^-, 14380-61-1; OBr^-, 14380-62-2; Br^-, 24959-67-9; $Cu_2(OH)_6^{2-}$, 64332-60-1.

References and Notes

(1) L. Thênard, *Ann. Chim. Phys.*, **9**, 51 (1818).
(2) M. W. Lister, *Can. J. Chem.*, **31**, 638 (1953).
(3) M. Krüger, *Pogg. Ann.*, **62**, 447 (1844).
(4) R. Scholder and V. Voelskow, *Z. Anorg. Allg. Chem.*, **266**, 256 (1951).
(5) J. S. Magee and R. H. Wood, *Can. J. Chem.*, **43**, 1234 (1965).
(6) A. Prokopcikas, *Liet. TSR Mokslu Akad. Darb., Ser. B*, 41 (1964).
(7) A. A. Sakharov, *Uch. Zap. Petrozavodsk. Gos. Univ.*, **14**, 76 (1966).
(8) L. A. McDowell and H. L. Johnston, *J. Am. Chem. Soc.*, **58**, 2009 (1936).
(9) L. Maleprade, *C. R. Hebd. Seances Acad. Sci.*, 979 (1937).
(10) L. Malatesta, *Gazz. Chim. Ital.*, **71**, 467 (1941).
(11) G. Beck, *Mikrochem. Ver. Mikrochim. Acta*, **38**, 1 (1951).
(12) G. Beck, *Mikrochem. Ver. Mikrochim. Acta*, **35**, 169 (1950).
(13) G. Beck, *Mikrochem. Ver. Mikrochim. Acta*, **39**, 22 (1952).
(14) P. K. Jaiswal and K. L. Yadva, *J. Indian Chem. Soc.*, **51**, 750 (1974).
(15) I. Hadinec, J. Jensovský, A. Línek, and V. Synecek, *Naturwissenschaften*, **47**, 377 (1960).
(16) D. W. Margerum, K. L. Chellappa, F. P. Bossu, and G. L. Burce, *J. Am. Chem. Soc.*, **97**, 6894 (1975).
(17) F. P. Bossu, K. L. Chellappa, and D. W. Margerum, *J. Am. Chem. Soc.*, **99**, 2195 (1977).
(18) D. W. Margerum, L. F. Wong, F. P. Bossu, K. L. Chellappa, J. J. Czarnecki, S. T. Kirksey, and T. A. Neubecker, *Adv. Chem. Ser.*, **No. 162**, 281–303 (1977).
(19) D. C. Olsen and J. Vasilekskis, *Inorg. Chem.*, **10**, 463 (1971).
(20) D. Meyerstein, *Inorg. Chem.*, **10**, 638, 2244 (1971).
(21) J. J. Bour and J. J. Steggerda, *Chem. Commun.*, 85 (1967).
(22) J. J. Bour, P. J. M. W. L. Birker, and J. J. Steggerda, *Inorg. Chem.*, **10**, 1202 (1971).
(23) G. C. Allen and K. D. Warren, *Inorg. Chem.*, **8**, 1895 (1969).
(24) P. T. Beurskens, J. A. Cras, and J. J. Steggerda, *Inorg. Chem.*, **7**, 810 (1968).
(25) A. Vogel, "Quantitative Inorganic Analysis", 3rd ed, Wiley, New York, N.Y., 1961.
(26) H. Galal-Gorchev and J. C. Morris, *Inorg. Chem.*, **4**, 899 (1965).
(27) B. G. Willis, J. A. Bittikofer, H. L. Pardue, and D. W. Margerum, *Anal. Chem.*, **42**, 1340 (1970).
(28) M. J. Milano, H. L. Pardue, T. Cook, R. E. Santini, D. W. Margerum, and J. M. T. Raycheba, *Anal. Chem.*, **46**, 374 (1974).
(29) C. Lin, D. B. Rorabacher, G. R. Cayley, and D. W. Margerum, *Inorg. Chem.*, **14**, 919 (1975).
(30) N. W. Alcock, D. J. Benton, and P. Moore, *Trans. Faraday Soc.*, **66**, 2211 (1970).
(31) T. A. Neubecker and D. W. Margerum, unpublished results.
(32) J. L. Kurtz and D. W. Margerum, unpublished results.
(33) A. Prokopcikas and J. Butkevicius, *Liet. TSR Mokslu Akad. Darb., Ser. B*, 31 (1964).
(34) R. F. Jameson and N. J. Blackburn, *J. Inorg. Nucl. Chem.*, **37**, 809 (1975).
(35) R. F. Jameson and N. J. Blackburn, *J. Chem. Soc., Dalton Trans.*, 534 (1976).
(36) G. I. Rozovskii, A. K. Misyavichyas, and A. Yu. Prokopshik, *Kinet. Katal.*, **16**, 402 (1975).

Contribution from the Department of Chemistry, West Virginia University, Morgantown, West Virginia 26506

Isokinetic Temperatures and Mechanisms of Metal Ion Promoted Hydrolyses of Amino Acid Esters

STEPHEN A. BEDELL and ROBERT NAKON*

Received August 3, 1977 AIC705888

The activation parameters of Cu^{2+}-, Ni^{2+}-, Zn^{2+}-, and Co^{2+}-promoted hydrolysis of ethyl *N,N*-diacetoxyglycinate (EGDA) as well as those of (methyl glycinato)iminodiacetatocopper(II) have been determined as well as the isokinetic temperature, 392 K. These data are compared to those for tetradentate Ni(II) chelate and metal–nitrilotriacetate (NTA) hydrolyses of methyl glycinate; β = 274 K. The different trends in metal ion promotion and thermodynamic behavior of the hydrolyses of M(EGDA) (enthalpy dependent) and $M(NTA)^-$ (entropy dependent) are discussed in terms of differing mechanisms. The possible significance of these data to biological systems is also discussed.

Introduction

Metal ion catalyzed hydrolysis of amino acid esters has been studied by a number of research groups[1-7] with hopes of elucidating the role of metal ions in corresponding biological systems. Three mechanisms have been proposed, two involving external attack of hydroxide ion on the carbonyl carbon which has been activated toward nucleophilic attack by the polarizing effect of the metal ion either via induction through a coordinated amine group or by direct interaction of the ester carbonyl oxygen with the metal. The third mechanism involves formation of a metal–hydroxo complex, followed by intramolecular attack by hydroxide ion. Previously, we established[7] an isokinetic relationship between Ni(II) chelate and metal–nitrilotriacetate promoted hydrolyses of methyl glycinate and that catalysis occurred via induction rather than direct metal interaction with carbonyl oxygen of the ester. A series